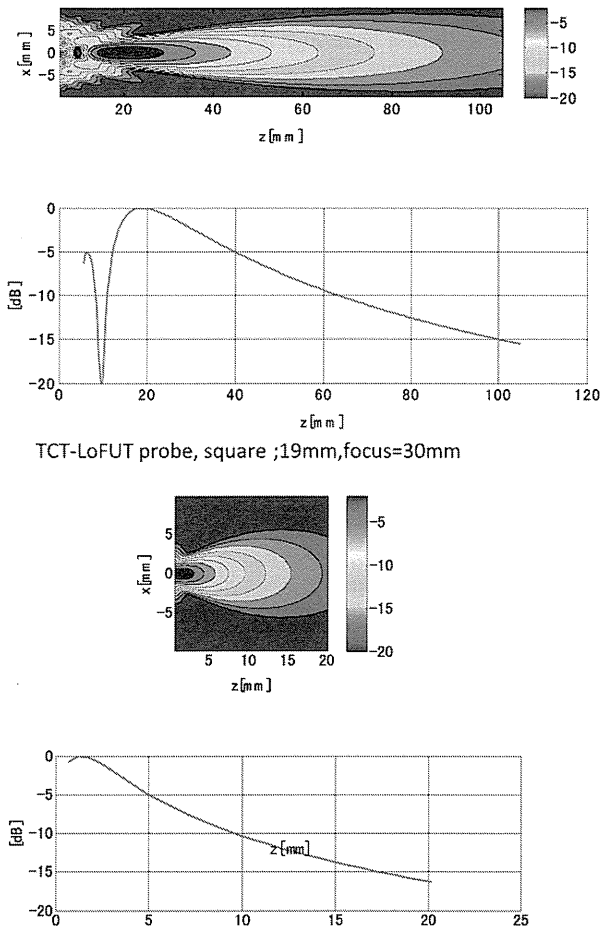

Fig. 7. Comparison of US beams between TCT-LoFUT and rat studies with 490-kHz CW-US. TCT-LoFUT can form a regular beam in front of the focus. The US beam for the rats extends as the distance increases, and the acoustic pressure falls.

Third, the large I_{SPPA} of BW-US with a PD >1.0 ms and a MI value >1.0 has great potential to induce cavitations in water (Wang et al. 2008). The actual PD in the TRUMBI trial was 2.0 ms at the focal point because four wide beams emitted from each transducer were gathered, and the PD of each beam was 0.5 ms.

Fourth, cavitation bubbles were trapped and retained in the brain tissue by a long-term standing wave caused by reflection at the inner surface of the cranium (Azuma et al. 2005).

Fifth, for BW-US with a large PD, the possibility of generating cavitation was determined by a new theoretical parameter, the eMI, the threshold of which was 3.0 (Appendix 1). In the TRUMBI trial, the intracranial eMI value was estimated to be 2.19 to 2.93 close to the cavitation threshold (Figure 8).

Before the TRUMBI trial, Daffertshofer et al. (2004) reported no increase in intracranial major bleeding caused by 25.57 kHz BW-US (I_{SPTA} 0.60 W/cm^2, DC 20%) with a high eMI value (5.61) in a rat MCA occlusion (MCAO) model under the rt-PA dosage. By contrast, after the failure of the TRUMBI trial, Nedelmann et al. (2008) reported on the use of 60 kHz BW-US (I_{SPTA} 0.14 W/cm^2, DC 50%) in a rat MCAO model receiving rt-PA. The overall mortality rate was higher in animals treated with BW-US, and histologic findings suggested disseminated microscopic ICH and subarachnoid hemorrhage as a possible cause of death. The eMI value in this BW-US condition was 1.12, which was the safety limit threshold for intracranial hemorrhage in BW-US and CW-US.

Saguchi et al. (2008) confirmed the lack of a bleeding effect in a rat MCAO model using 490 kHz CW-US in a TCT-LoFUT with an eMI value of 0.66. However, in terms of the safety limit, the LFUS beam used in the rat experiments differed notably from the beams used for humans, such as in the TCT-LoFUT (Fig. 7).

It was therefore considered dangerous to apply the safety limit of eMI obtained from small-animal experiments to species with larger craniums including humans.

It was therefore imperative that the safety limits be investigated in the larger-brained monkeys before clinical application of the TCT-LoFUT.

Recently, Deffieux et al. (2010) estimated the acoustic properties at low-frequency US (0.3 to 1MHz) through the occipital bone of human and rhesus monkeys using computed tomography–based acoustic maps of the cranium. They reported that 500-kHz US provided the best tradeoff between phase aberrations and standing wave effects in the human cranium, whereas 800-kHz US is the most suitable for the primate cranium. Consequently, focusing on the intracranial standing wave, our primate study was conducted as a potentially severe test for monkey brain using the 490-kHz CW-US.

A missing link of differences in adverse effects between clinical trial TRUMBI in BW-US and animal experiment in CW-US can be speculated by the eMI value mentioned later.

Using the measured transcranial US penetration ratio, the calculated intracranial eMI value for 494-kHz CW-US in the cynomolgus monkey was 0.42 at mean (Table 1).

Figure 8 shows the calculated intracranial eMI values through human temporal bone with thicknesses ranging from 2.0–5.0 mm, assuming an attenuation rate of 42–68% at 300-kHz US and 35–45% at 490-kHz US by calculation from a coefficient of 27.8 dB/cm/MHz, which was derived from the several previous reports (Ammi et al. 2008; Hölscher et al. 2008; Pfaffenberger et al. 2005). Accordingly, if the TCT-LoFUT was applied to the human cranium at the maximum permissible input intensity of 0.72 W/cm^2, the intracranial eMI value would

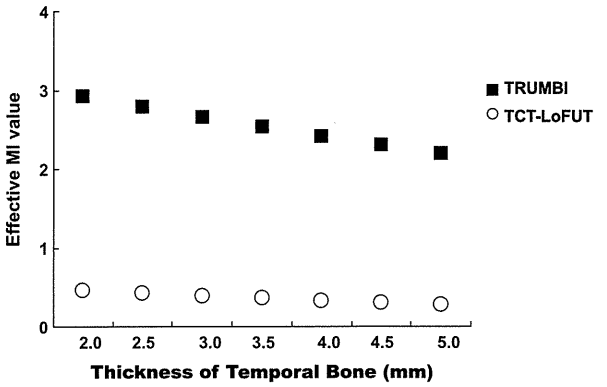

Fig. 8. Comparison of intracranial eMI values for human brains based on temporal bone penetration between TCT-LoFUT and the TRUMBI trial US conditions. The transcranial US penetrating ratio was calculated from the previously reported attenuation rate in the human skull (27.8 dB/MHz/cm).

range from 0.32–0.51, which is lower than or equivalent to that of the monkeys (Table 1). In other words, the eMI values at the maximum input intensity suggest that the TCT-LoFUT sonication could be applied with adequate safety to AIS patients for the clinical treatment of sonothrombolysis, because the eMI value for TCT-LoFUT would be lower than that shown to cause no US damage in monkeys.

The calculated intracranial MI value in the TRUMBI trial ranged from 0.73–0.98; therefore, the eMI value ranged from 2.19–2.94. The BW-US wave number reached 5, which showed high potential for inducing the cavitation effect (Holland et al. 1989). Midfrequency US has great potential for treating transcranial sonothrombolysis; however, its application under incorrect acoustic conditions could cause severe brain damage.

This experiment is a prudent first step before clinical application. Our next challenge is to inspect the safety of the CW-US used in the TCT-LoFUT in ischemic primate brains for clinical application of this innovative equipment in the future.

Acknowledgments—This study was supported in part by Health and Labor Sciences Research Grants from the Ministry of Health, Labor, and Welfare of Japan. The authors thank Masashi Kaburagi, Tomoko Yokota and Yoshikazu Sawaguchi, Ph.D., for their help in performing the experiments.

REFERENCES

Alexandrov AV, Molina CA, Grotta JC, Garami Z, Ford SR, Alvarez-Sabin J, Montaner J, Saqqur M, Demchuk AM, Moyé LA, Hill MD, Wojner AW, CLOTBUST Investigators. Ultrasound-enhanced systemic thrombolysis for acute ischemic stroke. N Engl J Med 2004;351:2170–2178.

American Institute of Ultrasound in Medicine. Mechanical bioeffects from diagnostic ultrasound. J Ultrasound Med 2000;19:73–168.

Ammi AY, Mast TD, Huang IH, Abruzzo TA, Coussios CC, Shaw GJ, Holland CK. Characterization of ultrasound propagation through ex vivo human temporal bone. Ultrasound Med Biol 2008;34: 1578–1589.

Azuma T, Kawabata K, Umemura S, Ogihara M, Kubota J, Sasaki A, Furuhata H. Bubble generation by standing wave in water surrounded by cranium with transcranial ultrasonic beam. J Jpn Appl Phys 2005;446B:4625–4630.

Azuma T, Ogihara M, Kubota J, Sasaki A, Umemura S, Furuhata H. Dual-frequency ultrasound imaging and therapeutic bilaminar array using frequency selective isolation layer. IEEE Trans Ultrason Ferroelectr Freq Control 2010;57:1211–1224.

Barnett HJM, Mohr JP, Stein BM, Yatsu FM. Stroke. Pathophisiology, diagnosis and management. 3rd ed. New York: Churchill Livingstone; 1998. 139–157, 649–700.

Barnett SB, Ter Haar GR, Ziskin MC, Rott HD, Duck FA, Maeda K. International recommendations and guidelines for the safe use of diagnostic ultrasound in medicine. Ultrasound Med Biol 2000;26: 355–366.

Baron C, Aubry JF, Tanter M, Meairs S, Fink M. Simulation of intracranial acoustic fields in clinical trials of sonothrombolysis. Ultrasound Med Biol 2009;35:1148–1158.

Behrens S, Spengos K, Daffertshofer M, Schroeck H, Dempfle CE, Hennerici M. Transcranial ultrasound-improved thrombolysis: Diagnostic vs. therapeutic ultrasound. Ultrasound Med Biol 2001; 27:1683–1689.

Daffertshofer M, Huang Z, Fatar M, Popolo M, Schroeck H, Kuschinsky W, Moskowitz MA, Gass A, Hennerici MG. Efficacy of sonothrombolysis in a rat model of embolic ischemic stroke. Neurosci Lett 2004;361:115–119.

Daffertshofer M, Gass A, Ringleb P, Sitzer M, Sliwka U, Els T, Sedlaczek O, Koroshetz WJ, Hennerici MG. Transcranial low-frequency ultrasound-mediated thrombolysis in brain ischemia: Increased risk of hemorrhage with combined ultrasound and tissue plasminogen activator: Results of a phase II clinical trial. Stroke 2005;36:1441–1446.

Deffeux T, Konofagou EE. Numerical study of a simple transcranial focused system applied to blood brain barrier opening. IEEE Trans Ultrason Ferroelectr Freq Control 2010;57:2637–2653.

Eggers J, Koch B, Meyer K, Konig I. Effect of ultrasound on thrombolysis of middle cerebral artery occlusion. Ann Neurol 2003;53: 797–800.

Eggers J, Ossadnik S, Seidel G. Enhanced clot dissolution in vitro by 1.8-MHz pulsed ultrasound. Ultrasound Med Biol 2009;35:523–526.

Fukuda T, Shimizu J, Furuhata H, Abe T, Shimizu K, Oishi T, Ogihara M, Kubota J, Sasaki A, Sasaki K, Azuma T, Umemura S. Overexpression of heat shock proteins in pallido-nigral axonal spheroids of nonhuman aged primates. Acta Neuropathol 2005;110:145–150.

Holland CK, Apfel RE. An improved theory for the prediction of microcavitation thresholds. IEEE Trans Ultrason Ferroelectr Freq Contr 1989;36:204–208.

Hölscher T, Wilkening WG, Molkenstruck S, Volt H, Koch C. Transcranial sound field characterization. Ultrasound Med Biol 2008;34: 937–980.

Ishibashi T, Akiyama M, Onoue H, Abe T, Furuhata H. Can transcranial ultrasonication increase recanalization flow with tissue plasminogen activator? Stroke 2002;33:1399–1404.

Leighton TG. The acoustic bubble. London: Academic Press, Hartcourt Brace & Company, 1994:377.

Molina CA, Ribo M, Rubiera M, Montaner J, Santamaria E, Delgado-Mederos R, Arenillas JF, Huertas R, Purroy F, Delgado P, Alvarez-Sabín J. Microbubble administration accelerates clot lysis during continuous 2-MHz ultrasound monitoring in stroke patients treated with intravenous tissue plasminogen activator. Stroke 2006;37:425–429.

Nedelmann M, Brandt C, Schneider F, Eicke BM, Kempski O, Krummenauer F, Dietrrich M. Ultrasound-induced blood clot dissolution without a thrombolytic drug is more effective with lower frequencies. Cerebrovasc Dis 2005;20:18–22.

Nedelmann M, Reuter P, Walberer M, Sommer C, Alessandri B, Schiel D, Ritschel N, Kempski O, Kaps M, Mueller C, Bachmann G, Gerriets T. Detrimental effects of 60kHz sonothrombolysis in rats with middle cerebral artery occlusion. Ultrasound Med Biol 2008;34:937–980.

Ogihara M, Kubota J, Azuma T, Ando K, Tanifuji Y, Umemura S, Furuhata H. Verification of ultrasonic thrombolysis effect by in vitro experiments. J Jpn Appl Phys 2006;45:4736–4739.

Pfaffenberger S, Devcic-Kuhar B, Kollmann C, Kastl SP, Kaun C, Speidl WS, Weiss TW, Demyanets S, Ullrich R, Sochor H, Wober C, Zeitlhofer J, Huber K, Groschl M, Benes E, Maurer G, Wojta J, Gottsauner-Wolf M. Can a commercial diagnostic ultrasound device accelerate thrombolysis? An in vitro skull model. Stroke 2005;36:124–128.

Prosperetti A. Application of the subharmonic threshold to the measurement of the damping of oscillating gas bubbles. J Acoust Soc Am 1977;61:11–16.

Reinhard M, Hetzel A, Krüger S, Kretzer S, Talazko J, Ziyeh S, Weber J, Els T. Blood-brain barrier disruption by low-frequency ultrasound. Stroke 2006;37:1546–1548.

Saguchi T, Onoue H, Urashima M, Ishibashi T, Abe T, Furuhata H. Effective and safe conditions of low-frequency transcranial ultrasonic thrombolysis for acute ischemic stroke. Neurologic and histologic evaluation in a rat middle cerebral artery stroke model. Stroke 2008;39:1007–1011.

Steen PA, Gisvold SE, Milde JH, Newberg LA, Scheithauer BW, Lanier WL, Michenfelder JD. Nimodipine improves outcome when given after complete ischemia in primates. Anesthesiology 1985;62:406–414.

Suchkova V, Carstensen EL, Francis CW. Ultrasound enhancement of fibrinolysis at frequencies of 27 to 100 kHz. Ultrasound Med Biol 2002;28:377–382.

Umemura S. Safety of ultrasound and therapeutic ultrasound. [In Japanese] Ultrason Technol (Tokyo, Nihon Kogyo Shuppan) 2004; 1:22–28.

Wang Z, Moehring MA, Voie AH, Furuhata H. In vitro evaluation of dual mode ultrasonic thrombolysis method for transcranial application with an occlusive thrombolysis model. Ultrasound Med Biol 2008;34:96–102.

Zenitani T, Suzuki R, Maruyama K, Furuhata H. Accelerating effects of ultrasonic thrombolysis with bubble liposome. J Med Ultrason 2008; 35:5–10.

APPENDIX

The formulae used for the calculations were as follows:

1. MI and eMI,

$$MI = (I \times \rho \times C \times 2)^{1/2} / f^{1/2} \text{ [MPa/MHz]}, \quad \text{(A1)}$$

where ρ is the density of water (10^3 kg/m^3) and C is the speed of sound in water (1.54×10^3 m/s), eMI = 3MI.

2. I_{SPPA} at BW-US,

$$I_{SPPA} = I_{SPTA} \times (1/DC\ [\%]) \times 100\ [\%]. \quad \text{(A2)}$$

Original Paper

Cerebrovascular Diseases

Cerebrovasc Dis 2012;33:23–29
DOI: 10.1159/000332034

Received: February 24, 2011
Accepted: August 15, 2011
Published online: November 30, 2011

Safety of Low-Frequency Transcranial Ultrasound in Permanent Middle Cerebral Artery Occlusion in Spontaneously Hypertensive Rats

Zuojun Wang[a, d] Takahiro Fukuda[b] Takashi Azuma[c] Hiroshi Furuhata[a]

[a]Medical Engineering Laboratory, [b]Division of Neuropathology, Research Center for Medical Sciences, Jikei University School of Medicine, and [c]Department of Biomedical Research, Faculty of Engineering, University of Tokyo, Tokyo, Japan; [d]Department of Ultrasonic Medicine, Tangdu Hospital, Fourth Military Medical University, Xi'an, China

Key Words

Acute stroke · Cerebral ischemia · Experimental stroke research · Intracranial hemorrhage · Hypertension · Thrombolysis · Ultrasound

Abstract

Background: Some studies suggest that low-frequency transcranial ultrasound (LFTUS) can enhance thrombolysis, but other studies suggest that it may have adverse effects on intracranial tissues. We previously reported that LFTUS with appropriate parameters was effective and safe in a normotensive rat model of thromboembolic middle cerebral artery occlusion (MCAO) stroke. The goal of this study was to test the safety of this strategy in a spontaneously hypertensive rat (SHR) model of permanent MCAO. ***Methods:*** Right MCAO was achieved in male SHRs using intraluminal nylon sutures. Rats exhibiting left hemiparesis were randomly assigned to one of four different groups: (1) normal saline (NS) group (n = 8), intravenous administration of NS as placebo at 3 h after MCAO; (2) NS+LFTUS group (n = 10), NS administration with simultaneous application of LFTUS (480.4 kHz, continuous wave, at an intensity of 0.3 W/cm^2) for 1 h; (3) tissue plasminogen activator (tPA) group (n = 11), intravenous administration of alteplase (10 mg/kg body weight) over 1 h instead of NS; or (4) tPA+LFTUS group (n = 11), tPA administration and application of LFTUS. Twenty-four hours after treatment, neurological change was evaluated, and brains were removed and examined histologically. ***Results:*** There was no significant difference ($p > 0.09$) when comparing changes in neurologic status and body weight, infarct ratio, edema ratio, or hemorrhagic transformation among the four groups. ***Conclusions:*** Our findings suggest that sonothrombolytic treatment with LFTUS with appropriate parameters is safe when used for the treatment of ischemic stroke in hypertensive rats under the undesired permanent MCAO condition.

Introduction

The thrombolytic efficacy of transcranial ultrasound in the treatment of acute ischemic stroke (AIS) [1–6] has attracted a great deal of attention among stroke investigators. Indeed, low-frequency ultrasound enhances the thrombolytic effect of other modalities [7–10] and has good skull penetration [11–13]. However, the TRUMBI trial demonstrated that low-frequency transcranial ultrasound (LFTUS) is associated with a very high rate of symptomatic intracranial hemorrhages in patients with AIS [14]. Studies performed to investigate the reasons for these complications [15–18] suggest that hemorrhage

KARGER

Fax +41 61 306 12 34
E-Mail karger@karger.ch
www.karger.com

1015–9770/12/0331–0023$38.00/0

Accessible online at:
www.karger.com/ced

Zuojun Wang, MD
Medical Engineering Laboratory
Jikei University School of Medicine
3-25-8 Nishi-shinbashi, Minato-ku, Tokyo 105-8461 (Japan)
Tel. +81 3 3433 1111, ext. 2338, E-Mail wangzj@jikei.ac.jp

may be related to a variety of factors, including intensity-dependent effects in the brain [15] and disruption of the blood-brain barrier [16].

These adverse effects of LFTUS may be dependent on the specific ultrasound settings. We previously reported that 490 kHz LFTUS with appropriate parameters was safe and effective in a normotensive Wistar rat model of middle cerebral artery occlusion (MCAO) [19]. However, hypertension is present in more than half of AIS patients [20]. Therefore, the goal of the present study was to determine whether LFTUS is safe in a spontaneously hypertensive rat (SHR) model of permanent MCAO.

Methods

All animal procedures were performed under the guidance of the animal research committee (Jikei University School of Medicine, Tokyo, Japan). Forty-five male, 12-week-old SHRs (Sankyo Labo Service Corp. Inc., Tokyo, Japan) were used in this study.

The rats were anesthetized via inhalation of isoflurane in air (4.8% for induction, 2.5% for surgery, and 1–2% for treatment) during both surgical and therapeutic procedures. Rectal temperature was maintained at 37.5 ± 0.5°C during all procedures with a thermal control blanket (BWT-100; BRC Co. Ltd., Nagoya, Japan).

Surgical Procedures

MCAO was achieved in SHR using a method modified from Koizumi et al. [21]. Briefly, under a surgical microscope, the right common, internal, and external carotid arteries were identified through a cervical midline incision. The external carotid artery and the occipital artery were ligated with a 4–0 silk suture. The internal carotid artery was temporarily closed with a Sugita aneurysm clip (temporary mini-type; Mizuho Ikagaku Industries, Tokyo, Japan), and the common carotid artery was closed using a suture 3-mm proximal to the carotid bifurcation. A small incision was made in the common carotid artery 1 mm proximal to the carotid bifurcation, and a 2–0 nylon suture was inserted from the common carotid artery into the internal carotid artery. After removing the Sugita clip, the suture was advanced 17–19 mm beyond the carotid bifurcation until mild resistance was felt. This resulted in occlusion at the origin of the MCA. Then, the cervical incision was closed and anesthesia was terminated.

Neurologic Evaluation and Body Weight Measurement

On a 5-point scale [22] (0 = no apparent deficits; 1 = contralateral forelimb flexion; 2 = decreased grip of the contralateral forelimb while tail pulled; 3 = spontaneous movement in all directions and contralateral circling only if pulled by tail; 4 = spontaneous contralateral circling), neurologic evaluation was blindly performed before surgery, just before treatment (3 h after MCAO) and at 24 h after treatment. Animals showing a neurologic score of 0 before surgery and a score of 3 or 4 before treatment were included in this study. The body weights of animals were also measured with an animal scale (SL-1000; A&D Co. Ltd., Seoul, Korea) at the time points described above.

Treatment Groups

Of the 45 rats used, 1 animal had a neurologic score of 0 before treatment, and we were unable to administer drug treatment intravenously in 4 animals. Thus, these animals were excluded from further study. Study animals (n = 40) were randomly assigned to one of the following four treatment groups: (1) normal saline (NS) group (n = 8), intravenous administration of NS as placebo via the tail vein (10 ml/kg body weight; 10% as a bolus, and the remainder infused over 60 min) at 3 h after MCAO; (2) NS+LFTUS group (n = 10), NS administration and application of LFTUS; (3) tissue plasminogen activator (tPA) group (n = 11), intravenous administration of tPA [alteplase (Mitsubishi Tanabe Pharma Corp., Osaka, Japan); 1 mg/ml, 10 ml/kg body weight; 10% as a bolus, and the remainder infused over 60 min] instead of NS; and (4) tPA+LFTUS group (n = 11), alteplase administration and application of LFTUS. The potency of human tPA in rats is approximately 10% of that in humans [23], i.e. a tPA dose of 10 mg/kg body weight in rats is equivalent to a therapeutic dose of tPA that is typically used for AIS in humans (0.9 mg/kg body weight).

Ultrasound System and Method

The ultrasound system utilized in this study has been described previously [19]. Briefly, the ultrasound transducer was custom-made for animal studies, with a plane circular surface of 5 mm in diameter and a resonant frequency of 480.4 kHz. The transducer was driven by a custom-made signal generator through a power amplifier (No. 4055; NF Corp, Yokohama, Japan) and a custom-made matching box. The transducer was set on the right scalp, centered 3 mm from the midline and 1 mm posterior to the bregma, with the help of a stereotaxic instrument (IMPACT-1000B; Muromachi Kikai, Tokyo, Japan). To enable better ultrasound transmission, the respective scalp area was depilated, and a layer of ultrasound gel was applied to the scalp before applying the transducer. Ultrasound conditions included a frequency of 480.4 kHz and spatial average intensity of 0.3 W/cm^2. Under this condition, the spatial peak intensity was approximately 1.2 W/cm^2, the mechanical index (MI) was 0.28, and the thermal index for the cranial bone was 2.9. Ultrasound output was confirmed with an ultrasound power meter (UPM-DT-1; Ohmic Instruments Co., Easton, Md., USA) before and after each treatment.

The ultrasound beam inside the rat cranial cavity was studied in a preliminary experiment using the schlieren method (fig. 1a) and the hydrophone (effective diameter, 0.2 mm) method (fig. 1b).

To avoid tissue heating, LFTUS was applied intermittently as previous described [19]. Briefly, after 2 min of continuous wave, irradiation was interrupted for 30 s. This pattern of application was repeated four times during a 10-min period, after which LFTUS was not performed for 5 min to enable cooling. These 10-min cycles of LFTUS, each followed by a 5-min break, were repeated four times over a period of 60 min.

Brain Extraction

After neurologic evaluation at 24 h after treatment, rats were deeply anesthetized with an intraperitoneal injection of 100 mg/kg of pentobarbital sodium (Somnopentyl; Kyoritsu Seiyaku Corp., Tokyo, Japan) and transcardially perfused with 50 ml of heparinized saline (5 U/ml) and 50 ml of 10% buffered formalin. Then, the brain, along with the front portion of the inserted nylon suture, was carefully extracted from the cranium. Photographs of brain surfaces and the intracranial cavity were taken to record the

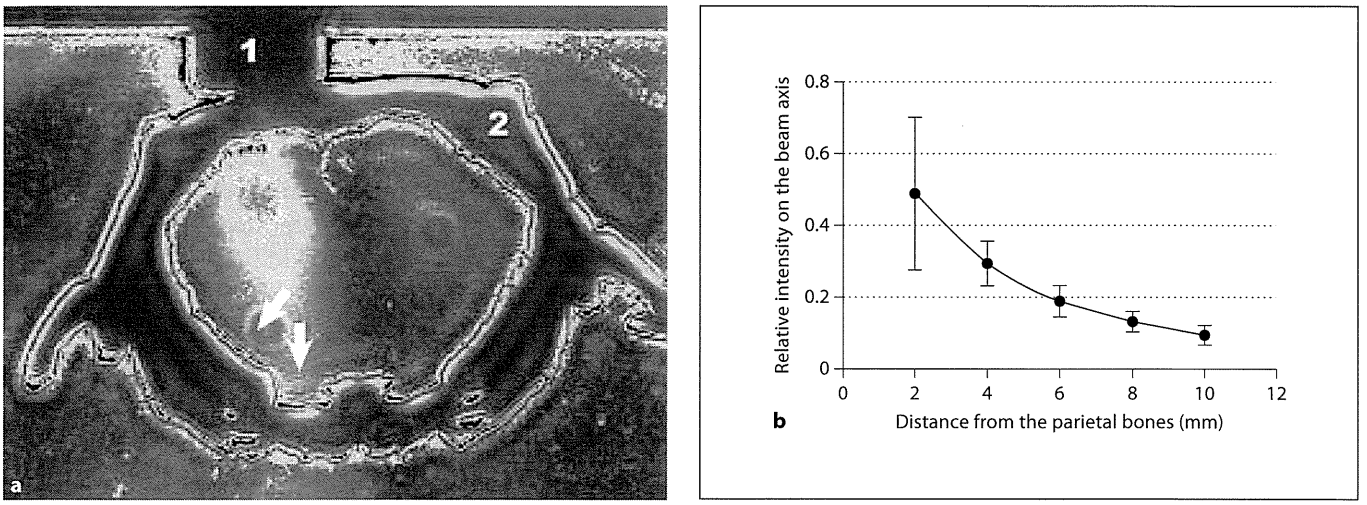

Fig. 1. a The ultrasound field inside a rat cranium observed with the schlieren method; 1 = LFTUS probe; 2 = rat cranium. The LFTUS probe was set on the parietal side of the rat cranium. The arrows indicate the formation of a standing wave as a striped pattern near the opposite side of the cranium. **b** The relative intensity of the LFTUS on the beam axis after its penetration through the parietal side of the rat cranium (n = 8).

position of the inserted suture and to document any visible abnormality on the brain and in the cranial cavity, including the potential presence of subarachnoid hemorrhage.

Cerebral Infarct and Edema Ratio

Each brain was cut into 2-mm-thick coronal sections. Six coronal sections (positioned 2–14 mm from the front pole) were obtained from each brain. Then, 3-μm thinly sliced specimens were prepared and stained with hematoxylin and eosin. Stained specimens were scanned with a flathead scanner (ES-8500; Seiko Epson Corp., Nagano, Japan) at a resolution of 3,200 dots per inch. The scanned images were analyzed with Photoshop image processing software. The infarct area in each section was measured as follows: (1) the infarct region was carefully selected in Photoshop with the lasso tool; (2) the pixel number of the selected region was determined in the histogram panel in Photoshop; and (3) the infarct area was determined by dividing the pixel number by the pixel density ($3,200 \times 3,200 = 10,240,000/inch^2 \approx 15,872/mm^2$). The infarct volume (IV) was calculated by summing the corresponding areas over all six sections and then multiplying the sum by the slice thickness (2 mm). The left hemisphere volume (LV) and the right hemisphere volume (RV) were determined in a similar manner. The edema ratio (ER) was calculated using the formula: $ER = (RV - LV)/LV \times 100\%$, and the edema-corrected infarct ratio (IR) was calculated using a formula similar to that proposed by Swanson et al. [24]: $IR = (LV - (RV - IV))/LV \times 100\%$.

Measurement of Intracerebral Hemorrhage

LFTUS has different field characteristics in the intracranial cavity (fig. 1), with the part near the parietal bone having stronger intensity and the part near the opposite cranium having a standing wave. Thus, intracerebral hemorrhage was examined at three different levels (i.e. 'near', 'middle', and 'far'; each occupying one third of the distance from the parietal side to the base side of the brain).

Hemorrhage was classified as macroscopic hemorrhage or microscopic hemorrhage. Macroscopic hemorrhage was defined as blood evident to the unaided eye on the hematoxylin and eosin-stained coronal sections and was graded according to its cross-sectional area (1: <0.8; 2: 0.8–3.1; 3: 3.1–7.1; 4: >7.1 mm^2) [25]. Microscopic hemorrhage was defined as a cluster of red blood cells outside of the lumen of blood vessels that could only be identified under microscopy [26]. Area of microscopic hemorrhage was measured with digital micrographs (4,116 × 3,072) taken with a ×20 objective lens of a Nikon biomicroscope (Eclipse 800-i) and summed for each level as well as for the whole hemisphere.

Statistical Analysis

Qualitative data (including neurologic score, mortality rate, subarachnoid hemorrhage rate, and macroscopic cerebral hemorrhage rate) were analyzed statistically using Fisher's exact test. Quantitative data (including body weight, IR, ER, and microscopic hemorrhage area) were presented as means ± SD and compared using one-way ANOVA. Differences with $p < 0.05$ were considered statistically significant.

Results

Mortality, Neurologic Score, and Body Weight Changes

One animal from the NS group died within 24 h of treatment. Neither subarachnoid hemorrhage nor significant intracerebral hemorrhage was found, but the ER (28.4%) was relatively high in this animal, which might

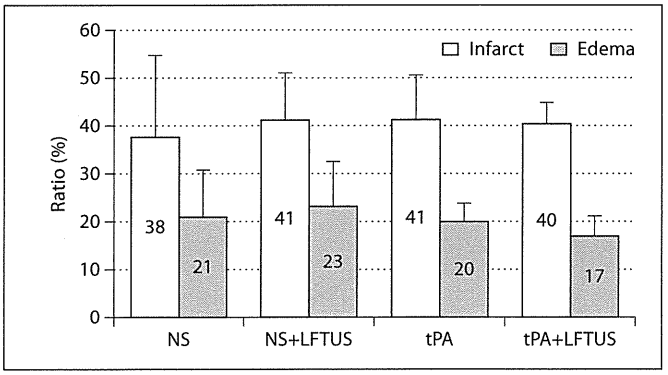

Fig. 2. Comparison of IR and ER. There was no significant difference among the four treatment groups in either of these indices.

have accounted for the mechanism of death. There was no significant difference in mortality rate ($p = 0.26$) among the four study groups. Nearly all animals had a neurologic score of 4 before treatment and a neurologic score of 3 at 24 h after treatment. There was no significant difference in neurologic score or change in body weight when comparing the four study groups.

Suture Position and Subarachnoid Hemorrhage

The inserted intraluminal suture was entered into the right anterior cerebral artery in all animals. Subarachnoid hemorrhage occurred in only one animal in the tPA group. There was no significant difference in the incidence of subarachnoid hemorrhage ($p = 0.45$) when comparing the four study groups.

Infarct Volume and Brain Edema

The IR was approximately 40%, and the ER was approximately 20% in all four study groups (fig. 2). There was no significant difference in IR ($p = 0.9$) or ER ($p = 0.25$) when comparing the four study groups.

Intracerebral Hemorrhage

Macroscopic hemorrhage occurred in 2 animals (1 in the NS+LFTUS group and 1 in the tPA group), both of which were in the 'middle' level (fig. 3) and were scored as grade 1 (i.e. area less than 0.8 mm^2). There was no significant difference in the macroscopic hemorrhage rate when comparing the four study groups (table 1). Microscopic hemorrhage measurements are also shown in the table. There was no significant difference in microscopic hemorrhage area when comparing the four study groups.

Discussion

This study found no significant difference among the four groups in any of the examined indices, including change in neurologic score, IR, ER, and hemorrhagic transformation. These results suggest that LFTUS is a safe therapeutic strategy in a hypertensive animal model of permanent occlusion. It should be noted that because this study explored the safety of LFTUS under the undesired permanent MCAO condition by using an indissoluble intraluminal suture to occlude the middle cerebral artery, it was unable to characterize any potential beneficial effects of ultrasound-mediated enhancement of thrombolysis, such as a decrease of infarct size [9] or alleviation of neurological score [19].

More than half of AIS patients have a history of hypertension [20], and hypertension is independently associated with poor outcome [27]. Therefore, many experimental studies of AIS, including those characterizing the therapeutic efficacy of tPA, utilize an SHR model of temporary MCAO [28]. However, nonrecanalization in response to clinical tPA treatment is not uncommon. Further, the TRUMBI trials showed that many symptomatic intracranial hemorrhages occurred in patients treated with LFTUS, who also had a low recanalization rate [14]. Therefore, the present study utilized an SHR model of permanent MCAO to test the safety of LFTUS.

The bleeding risk of thrombolytic treatment is closely related to (delayed) recanalization [25]. In Koizumi's permanent MCAO model, the thrombolytic effect of tPA is limited to the freshly formed thrombus around the suture in the occluded vessels, and the intraluminal suture cannot be dissolved to result in recanalization. Therefore, this model cannot evaluate the bleeding risk associated with (delayed) thrombolytic recanalization. However, one of the most important potential risks of the combined treatment of LFTUS with or without tPA may be its direct adverse effect on the disease or even healthy cerebral vessels [14]. In this context, use of Koizumi's MCAO model may be more appropriate than other models for the purposes of separating such direct adverse effects from those caused indirectly by thrombolytic recanalization.

This study demonstrated that sonothrombolysis with LFTUS was safe when used as late as 3 h after permanent MCAO in SHR. We propose that the safety of LFTUS is related to several different factors. First, LFTUS utilized in the present study had a low MI. In fact, with a continuous wave and a spatial average intensity of 0.3 W/cm^2, the corresponding spatial peak intensity was only about 1.2 W/cm^2, and the MI was only about 0.28. Thus, the MI

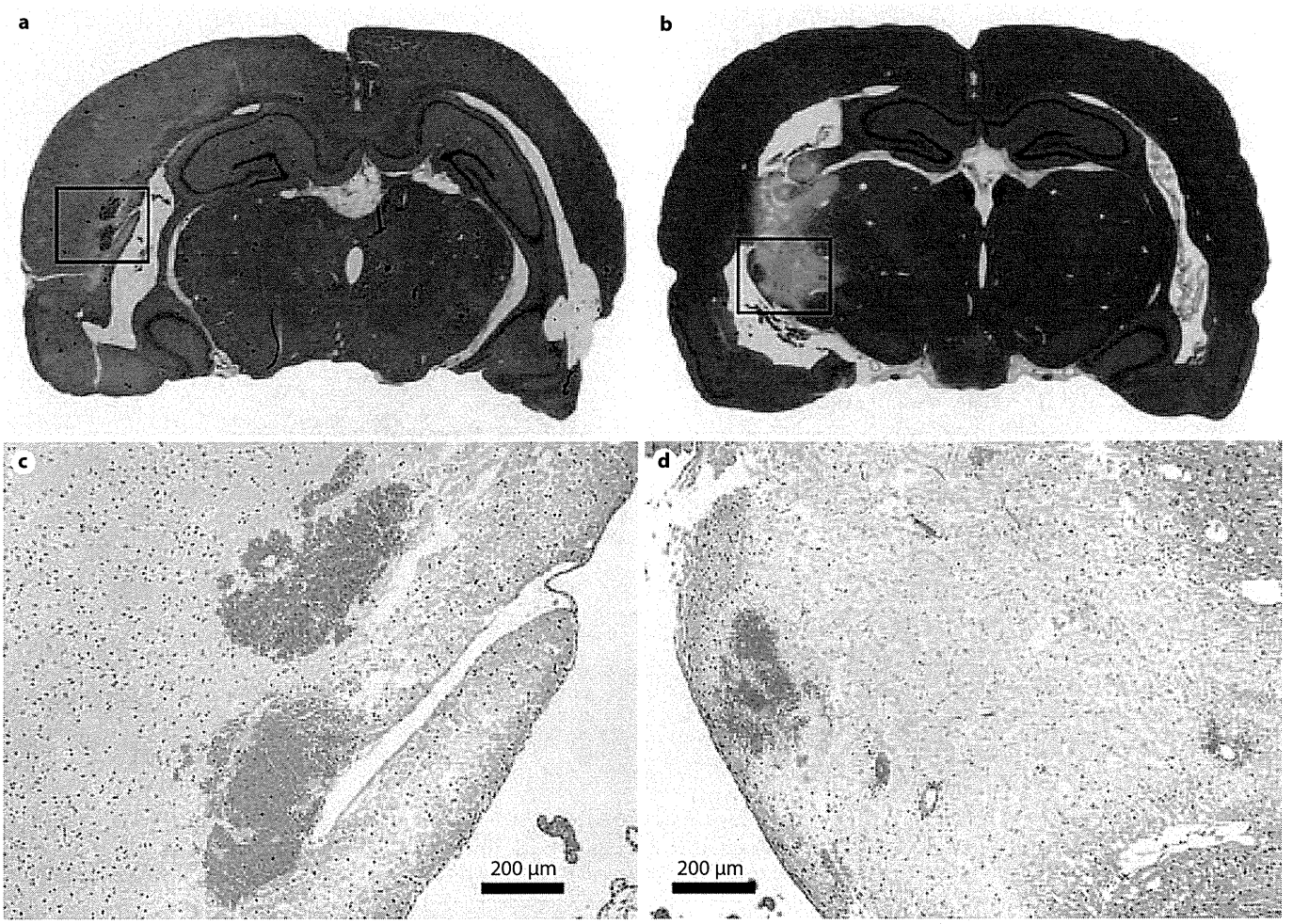

Fig. 3. Photographs of hematoxylin and eosin-stained rat brains of the 2 cases of macroscopic intracranial hemorrhages occurring in the tPA group (**a**) and the NS+LFTUS group (**b**). **c**, **d** Photomicrographs of the enclosed areas in **a** and **b**, respectively. Both macroscopic intracranial hemorrhages located in the 'middle' level of brain suggest little relationship with the applied TUS, of which intensity was stronger at the 'near' level and standing waves mainly occurred at the 'far' level.

Table 1. Intracerebral hemorrhages

Groups	Macroscopic hemorrhage rate (%)				Microscopic hemorrhage area ($\times 10^2$ μm^2)			
	near	middle	far	sum	near	middle	far	sum
NS (n = 8)	0	0	0	0	35 ± 78	103 ± 76	81 ± 81	219 ± 188
NS+LFTUS (n = 10)	0	10	0	10	111 ± 192	148 ± 276	186 ± 187	445 ± 383
tPA (n = 11)	0	9	0	9	160 ± 361	116 ± 378	116 ± 143	392 ± 578
tPA+LFTUS (n = 11)	0	0	0	0	160 ± 179	87 ± 235	175 ± 247	368 ± 356
p value	1.00	0.84	1.00	0.84	0.73	0.75	0.61	0.65

was maintained within the biological effect threshold (MI = 0.5) [29], much lower than that used in the TRUMBI trial (MI = 1.2) and that used in animal experiments performed by Schneider et al. [15]. Second, the LFTUS utilized in the present study had a well-controlled beam aperture (only about 20 mm^2). The transducers used in the TRUMBI trial [14] had a total area of about 2,830 mm^2, which is about 18-fold of that ($\approx$150 mm^2) of a conventional clinical transcranial Doppler ultrasound transducer. In addition, the transducers used in the animal experiments by Schneider et al. [15] and by Reuter et al. [18] were also relatively large (350 mm^2, about 17.5-fold higher than the LFTUS in the present study). These large transducers result in delivery of much more acoustic energy into the intracranial cavity and increase the formation of dangerous standing waves near the opposite cranium [10, 30]. Third, the frequency ($\approx$500 kHz) of our LFTUS was higher than those used in other LFTUS studies (e.g. 300 kHz in the TRUMBI trial and 20 kHz in the study by Schneider et al. [15]). An excessively low frequency may increase the MI at the same spatial peak intensity [29] and result in excessively long penetration distance, increasing multireflection and interference of ultrasound waves within the cranium [10].

In conclusion, we previously demonstrated the safety and efficacy of our LFTUS in a normotensive Wistar rat model of thromboembolic MCAO. The present study demonstrated the safety of this strategy in an SHR model of permanent MCAO. However, because serious intracranial hemorrhages may occur more easily when recanalization occurs, further study of the safety of LFTUS in a clinically relevant hypertensive model of temporary occlusion model is necessary.

Acknowledgement

This work was supported by grant H21-008 for research on advanced technology from the Ministry of Health, Labor, and Welfare of Japan.

Disclosure Statement

The authors declare that they have no conflicts of interest.

References

1 Alexandrov AV, Molina CA, Grotta JC, Garami Z, Ford SR, Alvarez-Sabin J, Montaner J, Saqqur M, Demchuk AM, Moye LA, Hill MD, Wojner AW, CLOTBUST Investigators: Ultrasound-enhanced systemic thrombolysis for acute ischemic stroke. N Engl J Med 2004;351:2170–2178.

2 Cintas P, Le Traon AP, Larrue V: High rate of recanalization of middle cerebral artery occlusion during 2-MHz transcranial color-coded Doppler continuous monitoring without thrombolytic drug. Stroke 2002;33:626–628.

3 Holscher T, Raman R, Ernström K, Parrish J, Le DT, Lyden PD, Mattrey RF: In vitro sonothrombolysis with duplex ultrasound: first results using a simplified model. Cerebrovasc Dis 2009;28:365–370.

4 Meairs S, Culp W: Microbubbles for thrombolysis of acute ischemic stroke. Cerebrovasc Dis 2009;27(suppl 2):55–65.

5 Molina CA, Ribo M, Rubiera M, Montaner J, Santamarina E, Delgado-Mederos R, Arenillas JF, Huertas R, Purroy F, Delgado P, Alvarez-Sabin J: Microbubble administration accelerates clot lysis during continuous 2-MHz ultrasound monitoring in stroke patients treated with intravenous tissue plasminogen activator. Stroke 2006;37:425–429.

6 Molina CA, Alvarez-Sabín J: Recanalization and reperfusion therapies for acute ischemic stroke. Cerebrovasc Dis 2009;27(suppl 1):162–167.

7 Nedelmann M, Eicke BM, Lierke EG, Heimann A, Kempski O, Hopf HC: Low-frequency ultrasound induces nonenzymatic thrombolysis in vitro. J Ultrasound Med 2002;21:649–656.

8 Suchkova V, Carstensen EL, Francis CW: Ultrasound enhancement of fibrinolysis at frequencies of 27 to 100 kHz. Ultrasound Med Biol 2002;28:377–382.

9 Daffertshofer M, Huang Z, Fatar M, Popolo M, Schroeck H, Kuschinsky W, Moskowitz MA, Hennerici MG: Efficacy of sonothrombolysis in a rat model of embolic ischemic stroke. Neurosci Lett 2004;361:115–119.

10 Wang Z, Moehring MA, Voie AH, Furuhata H: In vitro evaluation of dual mode ultrasonic thrombolysis method for transcranial application with an occlusive thrombosis model. Ultrasound Med Biol 2008;34:96–102.

11 Akiyama M, Ishibashi T, Yamada T, Furuhata H: Low-frequency ultrasound penetrates the cranium and enhances thrombolysis in vitro. Neurosurgery 1998;43:828–832.

12 Behrens S, Daffertshofer M, Spiegel D, Hennerici M: Low-frequency, low intensity ultrasound accelerates thrombolysis through the skull. Ultrasound Med Biol 1999;25:269–273.

13 Behrens S, Spengos K, Daffertshofer M, Schroeck H, Dempfle CE, Hennerici M: Transcranial ultrasound-improved thrombolysis: diagnostic vs. therapeutic ultrasound. Ultrasound Med Biol 2001;27:1683–1689.

14 Daffertshofer M, Gass A, Ringleb P, Sitzer M, Sliwka U, Els T, Sedlaczek O, Koroshetz WJ, Hennerici MG: Transcranial low-frequency ultrasound-mediated thrombolysis in brain ischemia: increased risk of hemorrhage with combined ultrasound and tissue plasminogen activator: results of a phase II clinical trial. Stroke 2005;36:1441–1446.

15 Schneider F, Gerriets T, Walberer M, Mueller C, Rolke R, Eicke BM, Bohl J, Kempski O, Kaps M, Bachmann G, Dieterich M, Nedelmann M: Brain edema and intracerebral necrosis caused by transcranial low-frequency 20-kHz ultrasound: a safety study in rats. Stroke 2006;37:1301–1306.

16 Reinhard M, Hetzel A, Kruger S, Kretzer S, Talazko J, Ziyeh S, Weber J, Els T: Blood-brain barrier disruption by low-frequency ultrasound. Stroke 2006;37:1546–1548.

17 Fatar M, Stroick M, Griebe M, Alonso A, Hennerici MG, Daffertshofer M: Brain temperature during 340-kHz pulsed ultrasound insonation: a safety study for sonothrombolysis. Stroke 2006;37:1883–1887.

18 Reuter P, Masomi J, Kuntze H, Fischer I, Helling K, Sommer C, Alessandri B, Heimann A, Gerriets T, Marx J, Kempski O, Nedelmann M: Low-frequency therapeutic ultrasound with varied duty cycle: effects on the ischemic brain and the inner ear. Ultrasound Med Biol 2010;36:1188–1195.
19 Saguchi T, Onoue H, Urashima M, Ishibashi T, Abe T, Furuhata H: Effective and safe conditions of low-frequency transcranial ultrasonic thrombolysis for acute ischemic stroke: neurologic and histologic evaluation in a rat middle cerebral artery stroke model. Stroke 2008;39:1007–1011.
20 O'Donnell MJ, Xavier D, Liu L, Zhang H, Chin SL, Rao-Melacini P, Rangarajan S, Islam S, Pais P, McQueen MJ, Mondo C, Damasceno A, Lopez-Jaramillo P, Hankey GJ, Dans AL, Yusoff K, Truelsen T, Diener HC, Sacco RL, Ryglewicz D, Czlonkowska A, Weimar C, Wang X, Yusuf S, INTERSTROKE Investigators: Risk factors for ischaemic and intracerebral haemorrhagic stroke in 22 countries (the INTERSTROKE study): a case-control study. Lancet 2010;376:112–123.
21 Koizumi J, Yoshida Y, Nakazawa T, Ooneda G: Experimental studies of ischemic brain edema I. A new experimental model of cerebral embolism in rats in which recirculation can be introduced in the ischemic area. Jpn J Stroke 1986;8:1–8.
22 Menzies SA, Hoff JT, Betz AL: Middle cerebral artery occlusion in rats: a neurological and pathological evaluation of a reproducible model. Neurosurgery 1992;31:100–106.
23 Korninger C, Collen D: Studies on the specific fibrinolytic effect of human extrinsic (tissue-type) plasminogen activator in human blood and in various animal species in vitro. Thromb Haemost 1981;46:561–565.
24 Swanson RA, Morton MT, Tsao-Wu G, Savalos RA, Davidson C, Sharp FR: A semiautomated method for measuring brain infarct volume. J Cereb Blood Flow Metab 1990;10:290–293.
25 Lu A, Clark JF, Broderick JP, Pyne-Geithman GJ, Wagner KR, Khatri P, Tomsick T, Sharp FR: Mechanical reperfusion is associated with post-ischemic hemorrhage in rat brain. Exp Neurol 2009;216:407–412.
26 Zhang L, Zhang ZG, Zhang RL, Lu M, Krams M, Chopp M: Effects of a selective CD11b/CD18 antagonist and recombinant human tissue plasminogen activator treatment alone and in combination in a rat embolic model of stroke. Stroke 2003;34:1790–1795.
27 Sare GM, Geeganage C, Bath PM: High blood pressure in acute ischaemic stroke – broadening therapeutic horizons. Cerebrovasc Dis 2009;27(suppl 1):156–161.
28 Gautier S, Petrault O, Gele P, Laprais M, Bastide M, Bauters A, Deplanque D, Jude B, Caron J, Bordet R: Involvement of thrombolysis in recombinant tissue plasminogen activator-induced cerebral hemorrhages and effect on infarct volume and postischemic endothelial function. Stroke 2003;34:2975–2979.
29 Apfel RE, Holland CK: Gauging the likelihood of cavitation from short pulse, low-duty cycle diagnostic ultrasound. Ultrasound Med Biol 1991;17:179–185.
30 Azuma T, Kawabata K, Umemura S, Ogihara M, Kubota J, Sasaki A, Furuhata H: Bubble generation by standing wave in water surrounded by cranium with transcranial ultrasonic beam. Jpn J Appl Physics 2005;44:4625–4630.

超音波は血栓成長を抑制する－塞栓成長抑制・再閉塞予防の可能性－

澤口　能一　　王　　作軍　　古幡　　博

Jpn J Med Ultrasonics Vol. 38 No. 5 別刷

超音波は血栓成長を抑制する －塞栓成長抑制・再閉塞予防の可能性－

澤口　能一　　王　　作軍　　古幡　　博

抄　録

目的：様々な血流再開通法において血栓再形成による再閉塞は非常に重要な問題である．そのため，新規超音波療法による血栓成長抑制を検証すべく，*in vitro* にてウシフィブリン血栓と中周波数超音波を用いて検討を行った．超音波による血栓成長抑制効果は超音波の音響強度ごとに定量的に評価を行った．**方法**：ウシ血漿に $CaCl_2$（最終濃度：25 mM）を直径 15 mm，高さ 1.5 mm の円盤状容器に入れ，37℃で 30 分間放置することで血栓を作製した．そこへ新たに血漿を加え密封した状態で 37℃の水浴中で 30 分間超音波を照射した．血栓成長抑制効果は分光光度計を用いて血栓の増高（mm）を定量化することで評価した．なお，本検討で使用した超音波照射条件は以下の通りである．周波数：500 kHz，音響強度：0.07－0.72 W/cm^2，振動子直径：10 mm，連続波．**結果と考察**：超音波照射群と超音波非照射群を比較した結果，音響強度 0.28－0.72 W/cm^2 において血栓成長を顕著に抑制出来ることを示した（$p<0.05$）．また，この血栓抑制効果は音響強度依存的に増強することが示唆された．**結論**：本検討で見出した低強度の中周波数超音波による新血栓成長抑制効果には，臨床的再開通法に伴う再閉塞リスクを低侵襲的に抑制出来る可能性があると期待された．

Ultrasound control of the growth of thrombus －potential for the embolus growth suppression & the reocclusion prevention－

Yoshikazu SAWAGUCHI, Zuojun WANG, Hiroshi FURUHATA

Abstract

Purpose: To prevent reocclusion after various recanalization therapies, we conducted an *in vitro* experiment using bovine fibrin clot and middle frequency ultrasonication to examine the ultrasonic therapeutic effect suppressing the regrowth of thrombi. Degree of ultrasonic control was quantitatively evaluated according to ultrasound (US) intensity. **Methods**: Discoidal clots created using bovine plasma with $CaCl_2$ (final concentration, 25 mM) at 37 degrees C in a circular container 15 mm in diameter and 1.5 mm deep. Fresh bovine plasma was placed on the clot after 30 minuets, and in an another container that was ultrasonicated for 30 minutes in a water bath at 37 degrees C. Growth rate was calculated by measuring change in clot thickness before and after sonication, from changes in optical absorption measured using a new precise optical system. Our new optical system utilized the relationship between spatial clot growth and US spatial intensity distribution on the discoidal clot. US conditions: frequency, 500 kHz; continuous wave intensity, 0.07 to 0.72 W/cm^2; and transducer diameter; 10 mm. **Results**: Suppression of thrombus growth was significantly greater in the US group than in the Non-US group, in which the controlled ratio increased over the intensity range of 0.28 to 0.72 W/cm^2 ($p<0.05$). **Conclusions**: These results suggest that a novel US control effect of thrombus regrowth with a middle frequency and low intensity can serve as a new noninvasive method for preventing thrombotic reocclusion in clinical risks caused by the various recanalization techniques.

Jpn J Med Ultrasonics 2011; 38(5): 549−555

Keywords

ultrasound, thrombus, reocclusion, prevention

1. はじめに

本邦死因第二位の心臓疾患の四割を占める心筋梗塞，同三位の脳血管障害の六割を占める脳梗塞は，いずれも血栓形成による血管閉栓状態が主原因である[1]．この血流途絶状態，すなわち組織へのライフラインの遮断状態を救済するために，急性期治療として血栓溶解療法やバルーンカテーテル，ステント留置などの経皮的血管形成術（PTA）による再開通法が適用されているが，治療後の血栓再形成による

東京慈恵会医科大学 ME 研究室
Medical Engineering Laboratory, Jikei University School of Medicine, 3−25−8 Nishi-shinbashi, Minato, Tokyo 105−8461 Japan
Received on 7 April, 2011; Revision accepted on 1 June, 2011

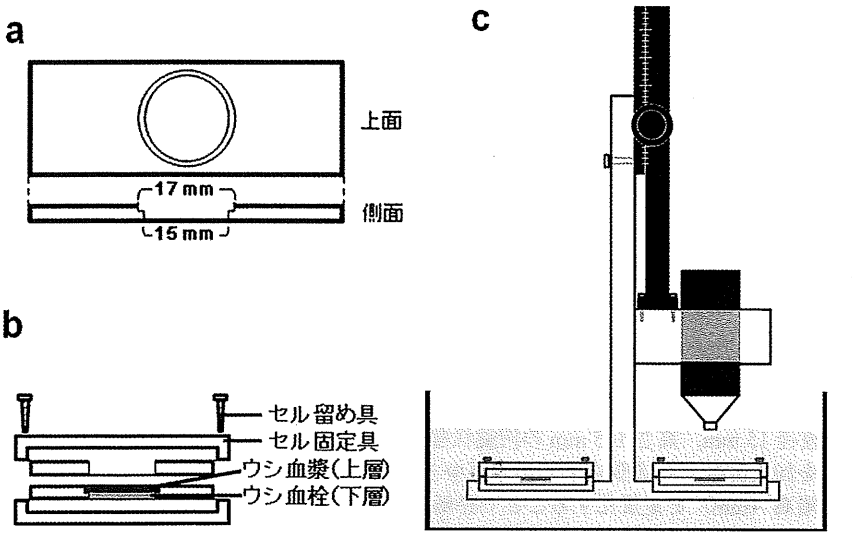

Fig. 1 血栓増加抑制実験容器概略図．**a** 血栓作製セル図面を示した．**b** 血栓上部に血漿を注入し，ポリカーボネート板で蓋をした後，血栓作製用セルを留め具で固定した．**c** 実際に超音波を照射する際の模式図を示した

再閉塞が問題となり[2-5]，各種抗血小板薬，抗凝固薬療法が施行されているのが現状である．また，凝血学的観点から，抗高脂血症薬などが適用され，一般的に言われる「血液さらさら」の予防的診療が行われていることも周知であろう．この様な血栓の発生からその成長，そして塞栓化を抑制するための薬学的療法に対し，物理的な効果を主体とする超音波による新規療法の可能性が考えられる．

超音波による血栓成長抑制効果については，すでに吉澤[6]によって犬大腿動脈血栓モデルを用いた非閉塞化実験で一部その有効性が示されている．彼らは大腿動脈内をバルーンカテーテルで内皮損傷させ，さらに血流を2時間遮断することで血栓形成により100%血管が閉塞される状態を作製し，その2時間の血流遮断中に200 kHzの超音波を照射し続けることで閉塞状態に至らず，血栓成長を抑制可能であると報告している．すなわち，音響力学的な振動作用によっても，血栓成長抑制が可能ではないかという成果を示している．しかし，それ以外に筆者らの知る限りにおいては，このような物理的血栓成長抑制法の報告はなく，またこの血栓成長抑制効果の定量的評価法についても不明であった．

本論文では，吉澤らと類似の500 kHz中周波数超音波照射条件下の *in vitro* 実験で，血栓成長抑制効果を定量的に評価した．

2. 方　　法

2.1 血栓作製

厚さ3 mmのアクリル板の上下よりそれぞれ1.5 mmずつ15 ϕ，17 ϕ の穴を空け，15 ϕ 側に0.3 mmのポリカーボネート板を張り付けたものを血栓作製セルとして用いた（**Fig. 1 a**）．この15 ϕの穴に，凍結乾燥ウシ血漿（sigma）を超純水で溶解したウシ血漿に対し，250 mM $CaCl_2$ を10%加えた（最終濃度：25 mM）溶液を270 μL注ぎ，湿潤させた密閉容器内で37℃，20分間放置することで，直径15 mm，深さ1.5 mmの円盤状血栓を作製した．

2.2 超音波照射条件

超音波照射台のプローブと血栓作製セルのステージの距離はダイヤルで任意に調整可能，かつプローブ（直径：10 ϕ）を血栓の中心軸上にしっかりと固定出来るようにデザインした（**Fig. 1 c**）．また，同時に超音波暴露血栓，非曝露血栓を同時に検討出来るようにした．超音波照射は，37℃の水槽内にプローブ先端を水面より2 mm程度沈め照射を行った．その際，超音波の反射を防ぐため，水槽底面には5 mmの超音波吸音材を敷き，さらにプローブと血栓の固定台自体を数度傾け，底面からの超音波の反射がセルに到達しないようにした．

超音波振動子の音場分布をAcoustic Intensity Measurement System（AIMS：Onda corporation,

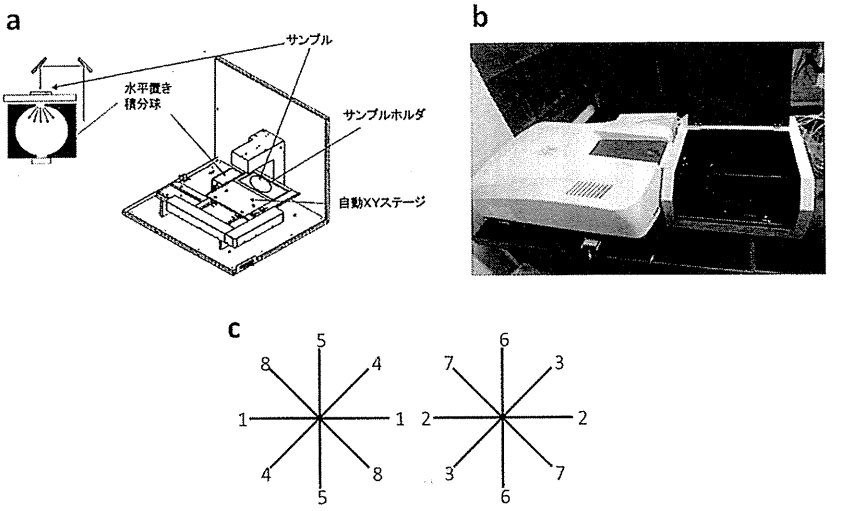

Fig. 2 血栓成長抑制の光学的評価．**a** 吸光光度計装置原理を示した．**b** 次に吸光光度計装置（日本分光：特注品）の写真を示した．**c** 吸光光度計による血栓2個同時測定の測定方向を示した．血栓は各測定方向に0.5 mm間隔で25点を測定し，血栓一つあたり計100点の吸光度を測定した

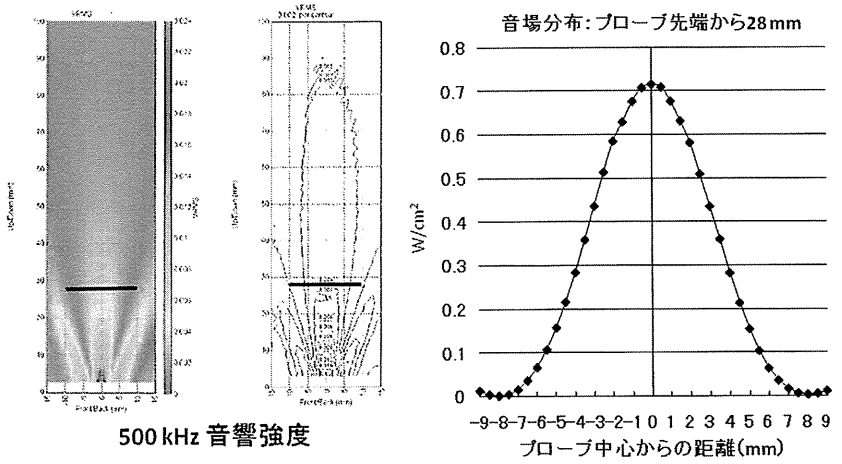

Fig. 3 超音波強度及び音場分布データ．音響強度測定装置AIMSにハイドロホンを設置して500 kHzの超音波プローブの水中における音響強度を測定し，またプローブから28 mm地点の音場分布を示した

Sunnyvale, CA）を用いて測定した．実測結果を**Fig. 3**に示した．この音場分布をもとに超音波振動子表面から血栓セルまでの距離を28 mmにセットした．この距離は，**Fig. 3**左図から明らかなように遠距離音場を呈する箇所である．その距離での音場断面は**Fig. 3**右図に示すように，中心より±8 mmの範囲内において一峰性の強度分布を示す箇所であった．実験は，同分布のピーク値，すなわち中心軸上の値をJIS基準における超音波診断装置の出力限界である0.72 W/cm^{2}となるように，駆動電圧を調整した．

2.3 血栓増加抑制実験

血栓上部の17 ϕの穴に新たにウシ血漿（400 μL）を注入し，0.3 mmのポリカーボネート板で気泡が入らないように十分に留意しながら蓋をした．このように血漿と血栓を直接接触させることで血栓を成長させた．この血栓成長状態の血栓を同時に二つ作製し，37℃の水浴中で一方は超音波を曝露，もう一方は超音波非曝露の状態で30分間放置した（**Fig. 1 c**）．その後，両者の血栓の成長の程度，すなわち円盤状血栓の厚さの差をもって，超音波による制御の程度を比較した．

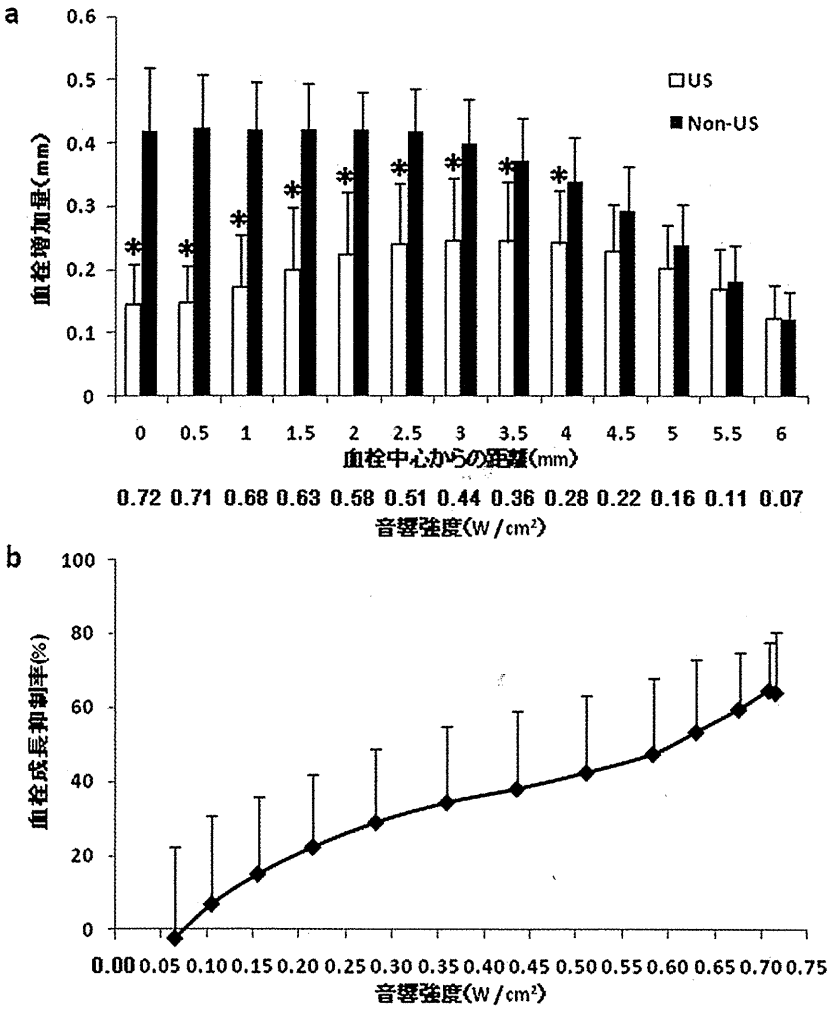

Fig. 4 超音波照射による血栓成長抑制．500 kHz の超音波を 30 分間照射し，血栓の成長が抑制出来るか否かを検討した．**a** 超音波照射前後での血栓増高量（mm）をグラフ縦軸，グラフ横軸上段には血栓中心からの距離，下段には血栓中心からの距離に対応する音響強度を示した．**b** また，各音響強度における血栓成長抑制率について示した．血栓成長抑制率は **Fig. 4 a** の血栓増加量（mm）の結果より，次式を用いて算出した“(ΔNon-US − ΔUS) / ΔNon-US”．$^{*}p < 0.05$ vs Non-US．mean ± SD．(n = 5)

2.4 血栓増加抑制作用の評価

超音波照射前後で血栓の吸光度（波長：412 nm）を測定した．血栓の増加量（mm）を，その吸光度の差から求めた．その際，吸光度と血栓の厚さで作製した検量線により厚さを換算した．円盤状の血栓の吸光度分布は，日本分光製（特注）の吸光度計を用いて，次のように自動計測された．円盤状血栓の中心を通る直径方向 25 点（中心から ± 6.0 mm, 0.5 mm 間隔）の吸光度（波長：412 nm）をまず自動計測した．続いて，この直径に対して 45° ずつ傾けた，3 方向の直径上の吸光度分布を同様に自動計測した（**Fig. 2**）．すなわち，8 方向の半径上の吸光度分布を測定したことになる．それゆえ，中心軸から等距離の値 8 点の平均値は，その距離における音響強度に対する平均吸光度とみなし，吸光度と血栓の厚さで作製した検量線により厚さを換算した．但し，中心（0 mm）のみ 1 点の吸光度の結果より評価した．

2.5 統計学的評価法

本実験では，円盤状血栓を 2 個ずつ 5 セット（計 10 個）用意し，2 個セットの一方を超音波曝露させ，非曝露側との血栓厚の差を Student t-test を用いて検定し，信頼度 95% をもって有意とした．

3. 結　　果

Fig. 4 a に超音波照射群及び非照射群血栓厚を示した．横軸は円盤状血栓の中心から 0.5 mm ごとの測定結果で，■は超音波非曝露時の血栓増加量（mm），□は超音波曝露時の血栓増加量（mm）である．各値は 5 セットの平均値と分散で各中心からの距離での血栓厚に有意差のある場合＊を付してある．図から明らかなように，中心から 4 mm の距離まで有意差を認め，超音波による血栓成長抑制効果が示された．この有意な差を示した中心からの距離を **Fig. 3** の音場データより音響強度に変換すると，音響強度 0.28－0.72 W/cm^2 の範囲になった．特に中心軸上では非曝露時の成長が約 0.4 mm であったのに対し，約 0.15 mm に抑制された．

音響強度と血栓成長抑制率の関係を **Fig. 4 b** に示した．図から明らかなように，音響強度依存的に血栓成長抑制率は上昇し，その曲線は僅かに S 字特性を示した．中でも，**Fig. 4 a** で統計学的に有意な値を示した強度閾値 0.28 W/cm^2 では，約 30％の抑制率となり，中心軸上の強度 0.72 W/cm^2 では約 64％となった．

4. 考　　察

本実験より，中周波数 500 kHz 連続波超音波には，約 0.3 W/cm^2 以上の音響強度であれば，強度依存的に血栓成長を抑制する効果を得られることを認めた．このような超音波による血栓成長抑制効果は，すでに 1992 年吉澤が行った *in vivo* 動物実験によって示されている[6]．すなわち，彼は犬両側大腿動脈の内皮をバルーンカテーテル擦過により損傷させ，バルーン抜去後さらに 2 時間血流を途絶することにより，処置例の全例（8/8）で血管が完全閉塞するモデルにおいて，片側に 200 kHz の連続波超音波を曝露し続けると，8 例中 7 例において『血管が閉塞しない』，という事実を報告している．この内皮損傷後に 2 時間結紮する血栓モデルは，血栓溶解の *in vivo* 実験の際に使われモデル系であり，血管閉塞の成功率はきわめて高いものであったが[7, 8]，この血栓形成時に超音波を照射し続けると，上述のように閉塞状態にならなかった，というものである．吉澤らは，そのメカニズムについて，定量的な考察を行っていなかった．本 *in vitro* 実験は，超音波に血栓成長抑制効果があることを定量的に示し，彼らの超音波による血管閉塞抑制のメカニズムを説明するものである．

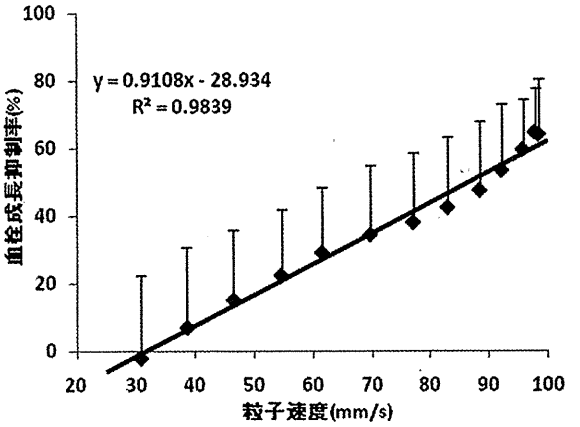

Fig. 5　粒子速度依存的な血栓成長抑制．**Fig. 4 b** の結果をもとに，横軸を音響強度より算出した粒子速度に変換して解析した．また，結果の散布図より得られる回帰直線ならびに近似式，決定係数（R^2）を算出した

血栓が超音波によって成長阻害される理由を我々は次の様なメカニズムであると考えている．超音波の分子作用を考える粒子速度 v（t）は，粒子速度の振幅（V），角周波数を（$2\pi f$），初期位相を（ϕ）を用いて，次式 $v(t) = V\sin(2\pi ft + \phi)$ で表わされる．この粒子速度の振幅（V）は，音響強度（I），密度（ρ），音速（c）を用いて，次式 $V = \sqrt{(2I/\rho c)}$ で表わされ，音響強度の増大と共に上昇するものである．**Fig. 5** に示すように，本検討において血栓成長抑制率と粒子速度（V）の回帰直線は線形を示し，その式は $R = KV - V_0$（R：血栓成長抑制率，K：比例定数，V_0：閾値）で表わすことができ，相関係数（R）は 0.992 と非常に高値を示した．このことから，第一義的には血栓成長抑制効果は粒子速度と比例関係にあると解釈され，この事実は，粒子速度が血栓へのフィブリンの結合を阻害する要因になっていると推察させるものである．この回帰直線から得られる血栓成長抑制作用の閾値は，粒子速度（V）では約 31.8 mm/s，本実験に用いたウシ血漿の密度（ρ）= 1.04 g/cm^2，血中の音速（c）= 1,540 m/sec を用いて音響強度に換算すると約 0.075 W/cm^2 となる．すなわち，超音波による血栓成長抑制作用は，この値以上であれば効果を発揮することを示唆するものである．一般に超音波の作用には粒子の振動作用だけでなく，“キャビテーション”や“発熱”といった作用が挙げられるが，本検討ではそれ

らの作用はほとんど影響しなかったと考える．その理由は，本実験で用いた超音波の最高音響強度は0.72 W/cm^{2}であり，キャビテーションの誘発に必要な音響強度（1 W/cm^2）には達しておらず，実際の実験中においても血栓セル内に目視での気泡は観察されなかったためである．また，周波数500 kHz，超音波出力0.72 Wの時の発熱作用を軟部組織のthermal index（TIS）に当てはめて算出すると約1.7を示すが，多量の水中に存在する厚さ1.5 mmの血栓の温度が実際に1.7℃も上昇するとは考え難いためである．

本実験での音響強度の値を血中で換算すると，音響強度I = 0.72 W/cm^{2}はV = 98.6 mm/s，有意な血栓成長抑制効果を示した最少強度0.28 W/cm^{2}ではV = 61.5 mm/sとなり，瞬時粒子速度が6 cmを超える振動を血漿に与えれば，自然な血栓成長を進める生化学作用を抑制出来ることが十分に考えられた．粒子速度は音圧あるいは音響強度に依存し，周波数に依存しないため，超音波による血栓成長抑制効果は本実験で用いた500 kHzに限らず，診断用の超音波（MHz帯）においても，類似の抑制効果を得ることが出来ると推察される．しかし，粒子速度が一定であった場合でも，実際に周波数を変化させると，その振動振幅は“$A = v/2\pi f$”より導かれるように粒子の振幅幅も変化させてしまう．この振幅幅の変化が血栓成長抑制効果に影響を与えるか否かについては現在のところデータを持ち合わせていないが，今後の検討で明らかになると考えられる．粘性流体のずり応力は周波数依存的であるので，血栓成長抑制作用には超音波の周波数依存特性が存在するものと考えられる[9]．この粘性成分を含む成長抑制作用及び診断用の超音波周波数帯など，他の周波数帯における抑制特性については，今後改めて検討を加えたい．従来，分子レベルでの音響的粒子速度が，生化学反応を阻害するという報告は，筆者らの知る限り存在せず，本実験結果は，ユニークな超音波作用を示している．

しかし，**Fig. 4 b**の血栓成長抑制率と音響強度の散布図の結果がS字状のうなりを示しており，血栓の固定具などの実験器具に超音波のサイドローブなどが反射し，実験結果に影響を及ぼした可能性が懸念される．それゆえ，超音波の反射の影響の有無についてより詳細に検証していくつもりである．また，本検討はウシ血漿を用いており，また吉澤の報告もイヌで示したものであるため，今後はヒト新鮮血を用いて検討を重ねるなど，臨床的実用化への実験を展開していく必要があると考えられる．

従来，血栓成長を阻害するには抗血小板薬，あるいは抗凝固薬などの生化学作用を持つ薬剤が適用されてきた[10-12]．そのため，これらの薬剤の血栓成長抑制能力と超音波による抑制能力との定量比較は，血栓成長抑制作用を評価する上で興味深く，本実験で使用した器具，条件を用いて試みるつもりである．

本論文で示した超音波固有の血栓成長抑制作用は，血管形成術後の血管再閉塞を回避する手段として，新たに物理的手法として介入出来る可能性が示唆された．さらには，狭心症や一過性脳虚血性発作（TIA）などに対しても（その主原因と考えられる塞栓状態に対して），予防的に超音波単独による経胸的，あるいは経頭蓋的照射による介入法が考えられる．この介入法について具体的な照射手法を示すことが出来る十分な検討は行っていないが，超音波の照射方法については，再閉塞が疑われる患部周辺で超音波プローブをバンドなどで固定して連続的に照射を行い，照射時間については，脳卒中のt-PA治療後2時間以内に再閉塞率が約20%[13]と報告されていることから少なくとも2時間以上の照射が必要になるであろうと考える．

5. 結　　語

超音波を照射するだけという非常にシンプルな方法で血栓成長を抑制し得ることを明らかにした．本論文で示した超音波血栓成長抑制作用は，新たな超音波予防技術の道を開く可能性があり，例えば虚血性疾患患者の予後における，2次予防に貢献する新規療法となることを期待する．

謝辞

本研究の一部は，厚生労働科学研究費補助金医療技術実用化総合研究事業「低侵襲的低周波超音波血栓溶解法の効果増高に関する臨床応用基礎研究」（課題番号：H21-トランス一般-008）の助成により遂行した．

文　　献

1) 厚生労働省．平成21年 人口動態統計月報年計（概数）の概況：死亡数・死亡率（10万人対），死因簡

単分類別 2010.
2) Harrison DG, Ferguson DW, Collins SM, et al. Rethrombosis after reperfusion with streptokinase: importance of geometry of residual lesions. Circulation 1984;69(5):991-9.
3) Collen D, Topol EJ, Tiefenbrunn AJ, et al. Coronary thrombolysis with recombinant human tissue-type plasminogen activator: a prospective, randomized, placebo-controlled trial. Circulation 1984;70(6):1012-7.
4) Roth C, Papanagiotou P, Behnke S, et al. Stent-assisted mechanical recanalization for treatment of acute intracerebral artery occlusions. Stroke 2010;41(11):2559-67.
5) Zhao L, Rubiera M, Hrrigan MR, et al. Arterial reocclusion and persistent distal occlusion after thrombus aspiration. J Neuroimaging 2010 Jun 21.
6) 吉澤直. 経皮的超音波照射による血栓溶解療法後の急性再閉塞予防効果に関する研究. 慈恵医大誌 1992;107:265-74.
7) 工藤澄彦. 超音波併用による血栓溶解療法に関する研究. 慈恵医大誌 1989;104:1005-12.
8) 浜野研司. 経皮的超音波照射併用による血栓溶解療法の有用性に関する研究. 慈恵医大誌 1991;106:533-42.
9) McDonald DA. Blood flow in arteries 2nd edition. Great Britain, Edward Arnold Ltd. 1974; p. 55-70.
10) Antithromboic Trialists' Collaboration. Collaborative meta-analysis of randomized trials of antiplatelet therapy for prevention of death, myocardial infarction, and stroke in high risk patients. BMJ 2002:12;324;71-86.
11) Antiplatelet Trialists' Collaboration. Collaborative overview of randomised trials of antiplatelet therapy-I: Prevention of death, myocardial infarction, and stroke by prolonged antiplatelet therapy in various categories of patients. BMJ 1994;308:81-106.
12) EAFT (European Atrial Fibrillation Trial) Study Group. Secondary prevention in non-rheumatic atrial fibrillation after transient ischaemic attack or minor stroke. Lancet 1993;342:1255-62.
13) Alexandrov AV, Molina CA, Grotta JC, et al. Ultrasound-enhanced systemic thrombolysis for acute ischemic stroke. N Enql J Med 2004;351:2170-8.

Carotid Duplex Ultrasonography Can Predict Outcome of Intravenous Alteplase Therapy for Hyperacute Stroke

Masatoshi Koga, MD, Kazunori Toyoda, MD, Takahiro Nakashima, MD, Boo-Han Hyun, MD, Toshiyuki Uehara, MD, Chiaki Yokota, MD, Kazuyuki Nagatsuka, MD, Hiroaki Naritomi, MD, and Kazuo Minematsu, MD

We evaluated whether carotid duplex ultrasonography (US) can help predict the safety and efficacy of treating hyperacute stroke with intravenous (IV) tissue plasminogen activator (alteplase) therapy. Consecutive patients with stroke were assigned to the carotid artery occlusion (CO) group or the other (non-CO) group according to US findings before or immediately after receiving IV alteplase. Effectiveness and safety outcomes included early neurologic improvement, defined as a reduction in a National Institutes of Health Stroke Scale (NIHSS) score of ≥4 points within the initial 24 hours after stroke onset; completely independent routine activity, defined as a modified Rankin Scale score of ≤1 at day 90 after stroke onset; symptomatic intracranial hemorrhage (ICH) occurring within 36 hours after stroke onset; and any ICH. We enrolled 127 patients (27 in the CO group and 100 in the non-CO group) with a median baseline NIHSS score of 13 (range, 4-30). The CO group had a higher baseline NIHSS score (median, 18 vs 12; $P = .005$). After multivariate adjustment, the CO group was inversely associated with early improvement (odds ratio [OR] = 0.26; 95% confidence interval [CI] = 0.09-0.72) and independence at day 90 (OR = 0.23; 95% CI = 0.05-0.73) and positively associated with any ICH (OR = 3.11; 95% CI = 1.23-8.48). Our findings indicate that CO identified by US in the emergency clinical setting is an independent predictor of unfavorable outcome and ICH following IV alteplase therapy. **Key Words:** Alteplase—internal carotid artery occlusion—intracranial hemorrhage—ultrasonography—outcome.

Occlusion of the internal carotid artery (ICA) often provokes severe hypoperfusion of cerebral blood flow in the affected territory. Patients who sustain acute ICA occlusion tend to have poor clinical outcomes.[1] Mortality is high in patients with malignant middle cerebral artery (MCA) infarction, resulting principally from distal ICA occlusion. The fates of patients with and without a major arterial occlusive lesion might differ after intravenous (IV) tissue plasminogen activator (alteplase) therapy, because resistance to clot lysis and the fragility of infarcted brain tissue may depend on the patency of the ICA. Rapid evaluation of arterial status in the emergency clinical setting may help predict outcome after alteplase therapy.

Magnetic resonance angiography (MRA) and computed tomographic angiography (CTA) can detect occlusions or severe stenoses of the cervicocephalic arteries supplying the infarcted area in patients with acute stroke,[2,3] as well as intracranial abnormalities with greater sensitivity and specificity, than conventional cerebral angiography.[3,4] Large ischemic lesions on diffusion magnetic resonance

From the Cerebrovascular Division, Department of Medicine, National Cardiovascular Center, Suita, Osaka, Japan.

Received August 17, 2009; revision received September 25, 2009; accepted October 2, 2009.

Supported in part by a Grant-in-Aid (H20-Junkanki-Ippan-019) from the Ministry of Health, Labor, and Welfare of Japan.

Address correspondence to Masatoshi Koga, MD, Cerebrovascular Division, National Cardiovascular Center, 5-7-1 Fujishirodai, Suita, Osaka 565-8565, Japan. E-mail: koga@hsp.ncvc.go.jp.

1052-3057/$ - see front matter

doi:10.1016/j.jstrokecerebrovasdis.2009.10.003

imaging (MRI) before IV alteplase therapy predict poor outcome in patients with acute ischemic stroke,[5] and diffusion–perfusion mismatch can select patients with remaining salvageable tissue.[6] But MRI takes at least 15 minutes, including equipment arrangement and patient transfer, to generate information, and CTA carries a risk of renal failure and anaphylaxis.

Carotid duplex ultrasonography (US) is another noninvasive tool that can detect major extracranial carotid arterial disease.[7-10] Compared with conventional cerebral angiography, US is not associated with such invasive complications as cerebral and systemic embolism, contrast agent anaphylaxis, acute renal dysfunction, and arterial dissection.[11] Morever, with bedside US, it takes only a few minutes to detect significant occlusive lesions of carotid arteries. US findings can help identify the mechanism and type of ischemic stroke.

We tested the hypothesis that carotid duplex US findings can help predict the outcome and safety of IV alteplase therapy for patients with hyperacute ischemic stroke.

Materials and Methods

We prospectively enrolled all patients with stroke who were admitted to our emergency stroke care unit and received IV alteplase therapy between October 2005 (when this therapy was approved in Japan) and July 2008. Our institution's Ethics Committee approved the research protocol. Patients or their representatives (eg, family members) provided written informed consent for the treatment.

Patient eligibility for IV alteplase therapy was based principally on the inclusion and exclusion criteria applied in the National Institute of Neurological Disorders and Stroke (NINDS) study[12] and in the Japan Alteplase Clinical Trial (J-ACT).[13] Each patient received a single IV dose of 0.6 mg/kg (not exceeding 60 mg) of alteplase, with 10% given as a bolus, followed by a continuous IV infusion of the remainder over 1 hour, in accordance with the Japanese guidelines for IV alteplase therapy based on the J-ACT results.[13,14] As in the NINDS study,[12] the use of antithrombotic agents were prohibited for 24 hours after onset, blood pressure was maintained at <180/105 mm Hg, and neurologic symptoms were monitored.

Clinical data included age and sex; time from symptom onset (or time when the patient last appeared to be normal) to the initiation of IV alteplase therapy; carotid artery US findings before or immediately after the initiation of alteplase therapy; National Institute of Health Stroke Scale (NIHSS) score immediately before (baseline) and 24 hours after alteplase therapy; concomitant diseases; current smoking and drinking habits; imaging data, including hemorrhagic transformation detected by computed tomography (CT) or MRI during hospitalization; stroke subtype according to Trial of Org 10172 in Acute Stroke Treatment (TOAST) criteria;[15] and modified Rankin Scale (mRS) score at day 90. Among concomitant diseases, hypertension was defined as systolic blood pressure ≥140 mm Hg or diastolic blood pressure ≥90 mm Hg before stroke onset or the use of antihypertensive medication. Diabetes was defined as preceding fasting blood glucose ≥126 mg/dL or the use of oral antidiabetic agents or insulin. Hypercholesterolemia was defined as total plasma cholesterol level ≥220 mg/dL or the use of antihypercholesterolemic medication.

Patients underwent US after hospitalization while awaiting the results of blood tests or immediately after starting alteplase therapy. US was performed with a bedside unit (Sonos 5500; Philips Medical Systems, Tokyo, Japan) with a 3- to 11-MHz linear transducer. On US, absent color flow signals on the ICA indicates the occlusion at or proximal to the artery, and absent end-diastolic flow velocity of the ICA indicates intracranial ICA occlusion.[16] Thus, carotid artery occlusion was defined as either of these US findings (Fig 1). Based on the US findings, the patients were divided into 2 groups: those with carotid artery occlusion (designated the CO group) and those without carotid artery occlusion (designated the non-CO group).

Before alteplase therapy, all patients underwent intracranial MRA to serve as the gold standard reference of carotid US findings, unless contraindicated. MRA was performed using the 3-dimensional time-of-flight technique (repetition time/echo time, 35/7.2 msec; 20-degree flip angle) with a 1.5 T system (Magnetom Vision; Siemens, Germany).

Outcomes included early neurologic improvement, defined as a ≥4-point reduction in NIHSS score within the initial 24 hours, and complete independence in activities of daily living (ADL), defined as an mRS score of 0 or 1, at 90 days. To assess long-term independence, patients with a mRS score of ≥2 before stroke onset were excluded. Safety outcomes included any intracranial hemorrhage (ICH) confirmed by head CT or MRI during hospitalization, and symptomatic ICH defined as early ICH with neurologic deterioration corresponding to a ≥1-point increase in the NIHSS score within 36 hours after alteplase therapy.

Statistical Analysis

Sensitivity, specificity, positive predictive value, and negative predictive value for detectng patients with carotid artery occlusion by carotid US were calculated when intracranial MRA findings were used as gold standard. Continuous and categorized variables were compared using the Student *t*-test and the χ^2 test, respectively. Nonparametric independent group comparisons were done using the Mann-Whitney *U*-test. To determine independent clinical variables to predict outcomes, significant variables were analyzed in a logistic regression model, with multivariate adjustments for age, sex, and confounders with an association of $P < .05$ with each outcome in univariate analysis. Statistical significance was established at $P < .05$.